Natalie J. Haywood, Paul A. Cordell, Kar Yeun Tang, Natallia Makova, Nadira Y. Yuldasheva, Helen Imrie, Hema Viswambharan, Alexander F. Bruns, Richard M. Cubbon, Mark T. Kearney, and Stephen B. Wheatcroft

Insulin-Like Growth Factor Binding Protein 1 Could Improve Glucose Regulation and Insulin Sensitivity Through Its RGD Domain

Diabetes 2017;66:287–299 | DOI: 10.2337/db16-0997

Low circulating levels of insulin-like growth factor binding protein 1 (IGFBP-1) are associated with insulin resistance and predict the development of type 2 diabetes. IGFBP-1 can affect cellular functions independently of IGF binding through an Arg-Gly-Asp (RGD) integrin-binding motif. Whether causal mechanisms underlie the favorable association of high IGFBP-1 levels with insulin sensitivity and whether these could be exploited therapeutically remain unexplored. We used recombinant IGFBP-1 and a synthetic RGD-containing hexapeptide in complementary in vitro signaling assays and in vivo metabolic profiling in obese mice to investigate the effects of IGFBP-1 and its RGD domain on insulin sensitivity, insulin secretion, and whole-body glucose regulation. The RGD integrin-binding domain of IGFBP-1, through integrin engagement, focal adhesion kinase, and integrin-linked kinase, enhanced insulin sensitivity and insulin secretion in C2C12 myotubes and INS-1 832/13 pancreatic β-cells. Both acute administration and chronic infusion of an RGD synthetic peptide to obese C57BL/6 mice improved glucose clearance and insulin sensitivity. These favorable effects on metabolic homeostasis suggest that the RGD integrin-binding domain of IGFBP-1 may be a promising candidate for therapeutic development in the field of insulin resistance.

Changes in 21st century lifestyle have led to an increased prevalence of obesity. In 2008, 1.46 billion adults worldwide were estimated to have a BMI of $\geq$25 kg/m^2; of these, 502 million were classified as obese (1). Obesity-related insulin resistance is a major cause of health disorders, including type 2 diabetes mellitus (T2DM) which is predicted to affect 300 million people worldwide by 2030 (2). T2DM is a major cause of arterial atherosclerosis, leading to premature myocardial infarction, stroke, and peripheral vascular disease (3). Disappointing results from clinical trials investigating a strategy of intensive blood glucose control to reduce cardiovascular events (4,5) highlight the need for novel approaches to reduce cardiovascular risk in individuals with T2DM.

Insulin-like growth factor binding proteins (IGFBPs) comprise a family of proteins that bind insulin-like growth factors (IGFs) with high affinity (6). Several IGFBPs possess distinctive structural motifs that allow interactions with cells or extracellular matrices and confer the ability of these proteins to signal independently of IGF binding (6). IGFBP-1 is a 30-kDa protein that is abundant in the circulation and is the most dynamically regulated of the IGFBPs as a consequence of inhibition of hepatic synthesis in relation to ambient insulin concentrations (7). Accordingly, short-term modulation of IGF-I bioavailability has been proposed as a potential mechanism implicating IGFBP-1 in glucose counterregulation (8). Cross-sectional studies in humans indicate a strong and consistent positive correlation between circulating IGFBP-1 concentrations and insulin sensitivity (9–16). In longitudinal studies, low baseline concentrations of IGFBP-1 strongly predict the subsequent development of incident diabetes (17–20). Negative correlations between IGFBP-1 and biomarkers of cardiovascular disease have also become apparent (9,15,21). We have previously reported that in vivo overexpression of IGFBP-1 in mice improves vascular insulin sensitivity, promotes nitric oxide production, lowers blood pressure, and protects against atherosclerosis

Division of Cardiovascular and Diabetes Research, Leeds Multidisciplinary Cardiovascular Research Centre, Faculty of Medicine and Health, University of Leeds, Leeds, West Yorkshire, U.K.

Corresponding author: Stephen B. Wheatcroft, s.b.wheatcroft@leeds.ac.uk.

Received 16 August 2016 and accepted 26 October 2016.

This article contains Supplementary Data online at http://diabetes.diabetesjournals.org/lookup/suppl/doi:10.2337/db16-0997/-/DC1.

(22). We also observed improved whole-body glucose tolerance and insulin sensitivity in these mice, but we did not investigate the molecular basis for these findings.

Interaction of the Arg-Gly-Asp (RGD) sequence of IGFBP-1 with the cell surface $\alpha_5\beta_1$-integrin has been identified as a mechanism by which IGFBP-1 can regulate cellular responses independently of IGF binding (23). IGF-independent actions of IGFBP-1 mediated by RGD-integrin interactions have been reported in several cell types, including Chinese hamster ovary cells, breast cancer cells, oligodendrocytes, and human dermal fibroblasts (23–26). However, whether IGFBP-1 exerts IGF-independent actions on cell types implicated in metabolic homeostasis remains unclear.

We hypothesized that IGFBP-1 through its RGD domain directly modulates insulin signaling and glucose regulation and therefore represents a potential novel therapeutic for insulin sensitization. We used complementary in vitro and in vivo assays to investigate the effects of IGFBP-1 and its RGD domain on insulin signaling, insulin-stimulated glucose uptake, glucose-stimulated insulin secretion, and metabolic homeostasis.

RESEARCH DESIGN AND METHODS

Cell Culture C2C12 Cells

C2C12 cells (a gift from K. White, University of Leeds) were cultured in growth media (DMEM 32430-100; Thermo Fisher Scientific) supplemented with 10% FCS. Differentiation was initiated by rinsing fully confluent cells once with PBS and adding differentiation media (DMEM supplemented with 5% FCS). The INS-1 832/13 cell line (a gift from R. Sivaprasadarao, University of Leeds) was cultured in growth media (RPMI medium R8758; Sigma-Aldrich) supplemented with 10% FCS, 10 mmol/L HEPES, 1 mmol/L sodium pyruvate, and 0.05 mmol/L 2-mercaptoethanol.

Recombinant Full-Length Human IGFBP-1 Expression

To construct the expression vector, the DNA coding sequence of the mature human IGFBP-1 polypeptide was amplified from IMAGE clone 4800940 using oligonucleotides 5′-GGTCGGCGCGTCTCCAGGTGCTCCGTGGCAG-3′ and 5′−GACAGAACATTATTTCATCTAGATTCAGTTTTGTAC-3′ and subcloned into pM-secSUMOstar vector using *Bsm*BI and *Xba*I sites. After subcloning, the coding sequence was verified by dideoxynucleotide DNA sequencing (Sequencing Services, University of Dundee). Site-directed mutagenesis of the pM-secSUMOstarIGFBP-1 plasmid was performed using the QuikChange Lightning kit (Agilent Technologies) using primers 5′-TCCAGAGATCTGGGGAGACCC-3′ and 5′-GGGTCTCCCCAGATCTCTGGA-3′ to generate a WGD R246W (mIGFBP-1) expression construct. For protein expression, Expi293F cells (Life Technologies) were transiently transfected with the expression vector using ExpiFectamine as detailed by the manufacturer's instructions, with medium harvested 7 days posttransfection. After removal of cells and cell debris by centrifugation (10 min at 300*g* then 10 min at 4,500*g*) and addition of protease inhibitor cocktail and phosphatase inhibitor cocktail 3 (both from Sigma), the medium was passed through a 0.2-μm filter, and protein was precipitated by the addition of two volumes saturated ammonium sulfate at 4°C followed by incubation on ice for 1 h. After centrifugation (4,500*g* at 4°C for 1 h), floating protein pellets were redissolved in Dulbecco PBS (DPBS), and residual ammonium sulfate was removed by gel filtration with DPBS-equilibrated Zeba gel filtration spin columns (Fisher Scientific). His_6 SUMO-IGFBP-1 fusion protein was then isolated using HisPur Cobalt spin columns (Fisher Scientific) as directed by the manufacturer's instructions. Eluates were buffer exchanged to DBPS using Zeba columns before digestion of His_6 SUMO-IGFBP-1 with SUMOstar Protease. Cleaved His_6 SUMOstar was removed with HisPur Cobalt spin columns, and eluent containing IGFBP-1 was applied to a Sephacryl S-100 column equilibrated with DPBS at room temperature using an ÄKTA avant chromatography system (GE Healthcare). Purity was confirmed to ≥95% by Coomassie staining of SDS-PAGE gels.

In Vitro Treatment for Signaling and Uptake Assays

Cells were serum starved overnight. Cells were pretreated with 500 ng/mL recombinant IGFBP-1 (rIGFBP-1), WGD-mutant IGFBP-1 (mIGFBP-1), RGD-containing hexapeptide (GRGDTP or RAD-containing control peptide GRADSP; Thermo Fisher Scientific) for 10 min. Cells were then were exposed to 100 nmol/L recombinant insulin (I9278; Sigma-Aldrich) for 10 min. For inhibitor assays, cells were exposed for 10 min and treated in media containing either 2.5 μmol/L integrin-linked kinase (ILK) inhibitor (407331; Calbiochem) or 100 nmol/L focal adhesion kinase (FAK) inhibitor (PZ0117; Sigma-Aldrich).

Immunoblotting

Cells were lysed using lysis buffer (FNN0011; Invitrogen) posttreatment. Lysates were clarified by centrifugation (13,000 rpm for 15 min). Fifty micrograms of total protein were separated by electrophoresis through 4–12% Bis-Tris gel (NP0335; Life Technologies) and blotted onto polyvinylidene fluoride membranes. Blots were probed with insulin receptor substrate 1 (IRS1) (2390; Cell Signaling), phosphorylated (p) IRS1 (Tyr608) (09-432; Millipore), protein kinase B (AKT) (9272; Cell Signaling), pAKT (Ser473) (4060; Cell Signaling), FAK (3285; Cell Signaling), pFAK (Tyr397) (8556; Cell Signaling), insulin receptor (IR) (3025; Cell Signaling), pIR (Tyr1162) (407707; Millipore), PCK1 (12940; Cell Signaling), α_5-integrin (sc-10729; Santa Cruz Biotechnology), β_1-integrin (sc-6622; Santa Cruz Biotechnology), and β-actin (Sc-47778; Santa Cruz).

Insulin-Stimulated Glucose Uptake Assay

After pretreatment with inhibitors, hexapeptide, and exposure to insulin, as previously described, 50 μg/mL 2-NBDG (N13195; Life Technologies) diluted in glucose-free medium was added for 15 min at 37°C. The 2-NBDG uptake reaction was stopped by removing the medium and washing the cells with PBS three times. Results were visualized on a microplate reader (Varioskan LUX; Thermo Fisher Scientific) at an excitation/emission maxima of ∼465/540 nm.

Glucose-Stimulated Insulin Secretion

INS-1 823/13 cells were washed with Hanks' balanced salt solution (HBSS) (144 mmol/L NaCl, 4.7 mmol/L KCl, 1.16 mmol/L $MgSO_4$, 2.5 mmol/L $CaCl_2$, 1.2 mmol/L KH_2PO_4, 25.5 mmol/L NaHCO, 20 mmol/L HEPES, 0.2% BSA, pH 7.2) and then left in HBSS for 2 h at 37°C. After 2 h, the secretagogues (3 mmol/L glucose used for basal insulin secretion level and 15 mmol/L glucose as stimulated level, supplemented with 500 ng/mL RGD or RAD hexapeptide and 2.5 μmol/L ILK inhibitor or 100 nmol/L FAK inhibitor) diluted in HBSS were added for 2 h at 37°C. After 2 h, the supernatant was removed and used in an ultrasensitive mouse insulin ELISA (90080; Crystal-Chem) per kit instructions.

Proliferation Assay

After a 2-h pretreatment with hexapeptide in high-glucose HBSS, INS-1 823/13 cells were used as a proliferation assay (C10337; Invitrogen) per kit instructions.

Animal Husbandry

Male C57BL/6 mice aged 7 weeks were purchased from Charles River Laboratories, U.K. Experiments were carried out under the authority of U.K. Home Office License PPL40/3523. Cages were maintained in humidity- (55%) and temperature-controlled (22°C) conditions with a 12-h light/dark cycle. To induce obesity, mice were fed a high-fat diet (D12492; Research Diets).

Chronic Infusion

Osmotic minipumps (1004; ALZET) filled with 100 μL of 10 mg/mL RGD or RAD hexapeptide were implanted subcutaneously under general anesthesia in 12-week-old C57BL/6 mice fed a high-fat diet for 4 weeks.

In Vivo Metabolic Studies

Mice were fasted for 16 h before glucose tolerance testing or for 2 h before insulin tolerance testing. Blood glucose was measured by using a hand-held glucose meter (Accu-Chek Aviva). An intraperitoneal injection of glucose 1 mg/g or recombinant human insulin 0.75 International Units/kg (Actrapid; Novo Nordisk, Bagsværd, Denmark) (supplemented with 50 μg of RGD or RAD control hexapeptide for acute studies) was administered. Glucose concentration was measured at 30-min intervals for 2 h from the point of glucose or insulin administration.

The indirect calorimetry measures were performed by the Vanderbilt Mouse Metabolic Phenotyping Center (MMPC) (DK-059637). Mice were individually placed in metabolic cages (identical to home cages with bedding) located in the Vanderbilt MMPC in a 12-h light/dark cycle temperature- and humidity-controlled room. Energy expenditure measures were obtained by using an indirect calorimetry system (Promethion; Sable Systems, Las Vegas, NV). Microperforated stainless steel air-sampling tubes located at the bottom of the cages were used to ensure that the cage air was sampled uniformly. Ambulatory activity and position were detected with XYZ beams and determined every second. The Promethion system uses a pull-mode, negative-pressure system with an excurrent flow rate set at 2,000 mL/min. Water vapor is continuously measured, and its dilution effect on O_2 and CO_2 are mathematically compensated for in the analysis stream. O_2 consumption and CO_2 production were measured for each mouse at 5-min intervals for 30 s. Incurrent air reference values were determined every four cages. The respiratory quotient was calculated as the ratio of CO_2 production over O_2 consumption. Energy expenditure was calculated by using the Weir equation (27): $\text{kcal/h} = 60 \times (0.003941 \times \text{VO}_2 + 0.001106 \times \text{VCO}_2)$ (Eq. 1).

Data acquisition and instrument control were coordinated by MetaScreen version 2.2.18 software, and the raw data were processed using ExpeData version 1.7.30 software (Sable Systems).

Hyperinsulinemic-euglycemic clamps were performed by the Vanderbilt MMPC (DK-059637). The Vanderbilt University Hormone Assay and Analytical Core performed the hormone analysis (DK-059637 and DK-020593). All procedures required for the hyperinsulinemic-euglycemic clamp were approved by the Vanderbilt University Animal Care and Use Committee. Catheters were implanted into a carotid artery and a jugular vein of mice for sampling and infusions, respectively, 5 days before the study as described by Berglund et al. (28). Insulin clamps were performed on mice fasted for 5 h by using a modification of the method described by Ayala et al. (29). [3-^{3}H]-glucose was primed (1.5 μCi) and continuously infused for a 90-min equilibration and basal sampling period (0.075 μCi/min). [3-^{3}H]-glucose was mixed with the nonradioactive glucose infusate (infusate-specific activity 0.5 μCi/mg) during the 2-h clamp period. Arterial glucose was clamped by using a variable rate of glucose (plus trace [3-^{3}H]-glucose) infusion, which was adjusted based on the measurement of blood glucose at 10-min intervals. By mixing radioactive glucose with the nonradioactive glucose infused during a clamp, deviations in arterial glucose-specific activity were minimized, and steady-state conditions were achieved. The calculation of glucose kinetics, therefore, was more robust (30). Baseline blood or plasma variables were calculated as the mean of values obtained in blood samples collected at −15 and −5 min. At time 0, insulin infusion (4 mU/kg body weight/min) was started and continued for 120 min. Mice received heparinized saline–washed erythrocytes from donors at 5 μL/min to prevent a fall in hematocrit. Blood was taken from 80 to 120 min for the determination of [3-^{3}H]-glucose. Clamp insulin was determined at 100 and 120 min. At 120 min, 13 μCi of 2[^{14}C]deoxyglucose ([^{14}C]2DG) was administered as an intravenous bolus. Blood was taken from 2 to 25 min for determination of [^{14}C]2DG. After the last sample, mice were anesthetized and tissues were freeze clamped for biochemical analysis. Plasma insulin was determined by radioimmunoassay. Radioactivity of [3-^{3}H]-glucose and [^{14}C]2DG in plasma samples and [^{14}C]2DG-6-phosphate in tissue samples were determined

by liquid scintillation counting. R_a and R_d were determined using steady-state equations (31). Endogenous glucose appearance was determined by subtracting the glucose infusion rate from total R_a. The glucose metabolic index was calculated as previously described (32).

IGFBP-1 plasma levels were measured by using an IGFBP-1 ELISA kit (ab100539; Abcam) per kit instructions. IGF-I levels were measured by using a Mouse/Rat IGF-I Quantikine ELISA Kit (MG100; R&D Systems) per kit instructions. Growth hormone plasma levels were measured by using a Mouse GH (Growth Hormone) ELISA Kit (E-EL-M0060; Elabscience) per kit instructions. Glucagon plasma levels also were measured by using a Mouse/Rat IGF-I Quantikine ELISA Kit (E-EL-M0555; Elabscience) per kit instructions.

Mass Spectrometry

Blood was collected from the lateral saphenous vein. Mass spectrometry analysis was performed by the Mass Spectrometry Facility, Faculty of Biological Sciences, University of Leeds.

Data Analysis

All data are shown as the mean ± SEM. Blots were analyzed with ImageJ software and normalized to a control on each blot to account for variation between unstimulated conditions per experimental replicate. Student unpaired *t* test was used for all statistical analyses and was performed with GraphPad Prism software.

RESULTS

rIGFBP-1 Enhances Insulin Signaling in C2C12 Skeletal Muscle Cells Through Its RGD Domain

Skeletal muscle represents the major insulin-responsive tissue responsible for glucose clearance. After binding of insulin, autophosphorylation of the IR activates a canonical signaling pathway that involves phosphorylation of critical signaling intermediaries, including IRS1 and AKT. We used immunoblotting to probe the effects of IGFBP-1 on insulin-stimulated phosphorylation of these critical nodes in the insulin signaling pathway in skeletal myocytes differentiated from the mouse C2C12 myoblast cell line. Preincubation with rIGFBP-1 caused a significant increase in insulin-stimulated AKT and IRS1 phosphorylation in C2C12 myotubes but did not affect phosphorylation of IR or the IGF-I receptor (IGF-1R) (Fig. 1*A–D*). In recognition that IGFBP-1 has been reported to modulate responses of other cells through the interaction of its RGD motif with $\alpha_5\beta_1$-integrin, we investigated whether a similar mechanism is responsible for the effects of IGFBP-1 on insulin signaling. We first confirmed that $\alpha_5\beta_1$-integrin is expressed in C2C12 myotubes (Supplementary Fig. 1). To determine whether the RGD domain of IGFBP-1 is required for enhancement of insulin signaling, we repeated these experiments in C2C12 myotubes preincubated with rIGFBP-1 subjected to site-directed mutagenesis to replace the RGD sequence with a whole-genome duplication (WGD) sequence, which is incapable of binding integrins (mIGFBP-1) (33). In contrast to the native protein, preincubation with mIGFBP-1 did not modulate insulin signaling (Fig. 1*E–H*), suggesting that the RGD sequence of IGFBP-1 is essential for insulin sensitization.

RGD Peptide Mimics rIGFBP-1–Enhanced Insulin Signaling in C2C12 Skeletal Muscle Cells

To determine whether the intact protein is required for IGFBP-1–mediated modulation of insulin signaling or whether the RGD sequence per se is sufficient to induce insulin sensitization, we performed experiments with an RGD synthetic hexapeptide. Preincubation of skeletal myotubes with the RGD peptide before insulin stimulation enhanced glucose uptake and mimicked the enhancement of AKT and IRS1 phosphorylation elicited by rIGFBP-1. Similar to IGFBP-1, the RGD peptide had no effect on pIR/IR or pIGF-1R/IGF-1R (Fig. 2*A–E*). A pretreatment with RAD control hexapeptide before insulin stimulation did not enhance glucose uptake by pAKT/AKT, pIRS1/IRS1, pIR/IR, or pIGF-1R/IGF-1R (Fig. 2*F–J*).

RGD Peptide–Enhanced Insulin Signaling in C2C12 Skeletal Muscle Cells Depends on FAK

Outside-in signaling after interaction of cell surface integrins with RGD is mediated by activation of intracellular signaling cascades in which FAK and ILK are believed to play critical roles (34,35). To investigate the downstream involvement of integrin signaling in the actions of the RGD hexapeptide, we repeated experiments in C2C12 myotubes using inhibitors of FAK and ILK. Inhibition of FAK completely prevented the augmentation of insulin-stimulated glucose uptake by RGD peptide (Fig. 3*A*). Similarly, inhibition of FAK prevented RGD-mediated augmentation of insulin-stimulated AKT and IRS1 phosphorylation (Fig. 3*B* and *C*). The effect of RGD peptide on FAK phosphorylation was determined through Western blot analysis of pFAK (Fig. 3*D*) and confirmed that RGD peptide pretreatment enhanced FAK activation. ILK inhibition had no significant effect on insulin-stimulated glucose uptake, or insulin-stimulated phosphorylation of AKT, IRS1, or FAK (Fig. 3*E–H*).

IGFBP-1 and RGD Peptide Do Not Phosphorylate IRS1, AKT, or FAK in the Absence of Insulin

To examine whether IGFBP-1 or RGD peptide per se directly lead to phosphorylation of signaling intermediaries, we carried out experiments in the absence of insulin stimulation. Incubation of C2C12 myotubes with rIGFBP-1 or RGD peptide had no significant effect on the insulin signaling pathway in the absence of insulin, although there was a modest trend for greater FAK and AKT phosphorylation in stimulated cells compared with unstimulated cells (Supplementary Fig. 2).

RGD Peptide Enhances Glucose-Stimulated Insulin Secretion in INS-1 823/13 Pancreatic β-Cells and Depends on Both FAK and ILK

A pancreatic β-cell line, INS-1 823/13, was used to investigate the effects of RGD hexapeptide on glucose-stimulated

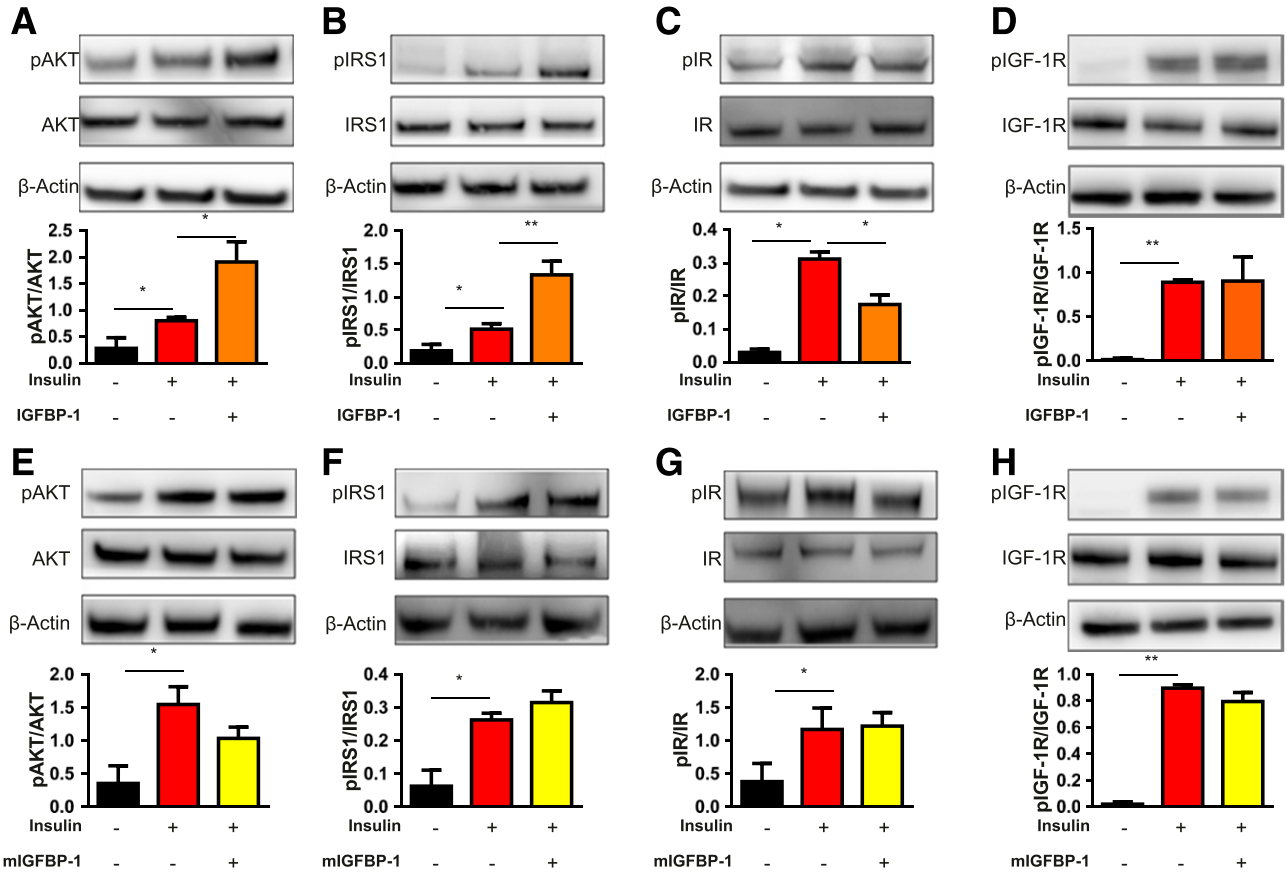

Figure 1—IGFBP-1 enhances insulin signaling through its RGD domain in C2C12 skeletal muscle cells. C2C12 myotubes were used to investigate the effects of rIGFBP-1 on the insulin signaling pathway through immunoblotting of key insulin signaling proteins (AKT, IRS1, IR, and IGF-1R). The relative intensities of phosphorylated and total protein bands were quantified by densitometry and expressed as a ratio (phosphorylated/total), normalized to β-actin. *A–D*: Pretreatment with 500 ng/mL rIGFBP-1 for 10 min before 100 nmol/L insulin stimulation for 10 min caused an increase in insulin-stimulated pAKT/AKT and pIRS1/IRS1 but not pIR/IR or pIGF-1R/IGF-1R compared with cells treated with insulin only. *E–H*: C2C12 myotubes were used to determine whether rIGFBP-1–enhanced insulin signaling was through its RGD domain by using a mIGFBP-1. Pretreatment with 500 ng/mL mIGFBP-1 for 10 min before 100 nmol/L insulin stimulation for 10 min had no effect on insulin-stimulated pAKT/AKT, pIRS1/IRS1, pIR/IR, or pIGF-1R/IGF-1R compared with cells treated with insulin only. Data are mean ± SEM. $^*P \leq 0.05$, $^{**}P \leq 0.01$ ($n = 3$).

insulin secretion. Incubation of INS-1 823/13 cells with RGD peptide in low-glucose conditions had no effect on insulin secretion compared with cells treated with low glucose only (Fig. 4*A*). However, incubation with RGD peptide significantly enhanced glucose-stimulated insulin secretion in INS-1 823/13 cells (Fig. 4*B*). RAD control peptide did not affect glucose-stimulated insulin secretion (Fig. 4*C*). Augmentation of glucose-stimulated insulin secretion by RGD peptide was blocked by inhibition of both FAK (Fig. 4*D*) and ILK (Fig. 4*E*). INS-1 823/13 cells were also used to investigate the effects of RGD peptide on pancreatic β-cell proliferation. RGD peptide incubation for 2 h enhanced INS-1 823/13 cell proliferation compared with cells treated with the RAD control peptide (Fig. 4*F*).

Acute RGD Peptide Treatment Has Beneficial Effects on Glucose Clearance and Insulin Sensitivity In Vivo

On the basis of the positive effect of the RGD hexapeptide on insulin signaling, cellular glucose uptake, and pancreatic insulin signaling observed in the preceding in vitro experiments, we proceeded to determine whether acute administration of RGD peptides modulated glucose regulation in vivo. Weight-matched C57BL/6 mice subjected to diet-induced obesity were used as an in vivo model of insulin resistance (Fig. 5*A* and *B*). Fifty micrograms of RGD peptide or RAD control peptide was administered to obese mice by intraperitoneal injection before metabolic profiling by glucose and insulin tolerance tests. Mass spectrometry analysis of plasma samples confirmed that the RGD peptide was detectable in the blood 30 min after injection (Fig. 5*C*). Multiple metabolites were also detected, suggesting partial protelytic degradation of the peptide. Administration of RGD peptide significantly improved glucose tolerance compared with administration of RAD control peptide (Fig. 5*D* and *E*). Insulin sensitivity was also significantly improved after administration of RGD peptide compared with RAD control peptide administration (Fig. 5*F* and *G*). A strong, although not statistically significant, trend for increased insulin-stimulated

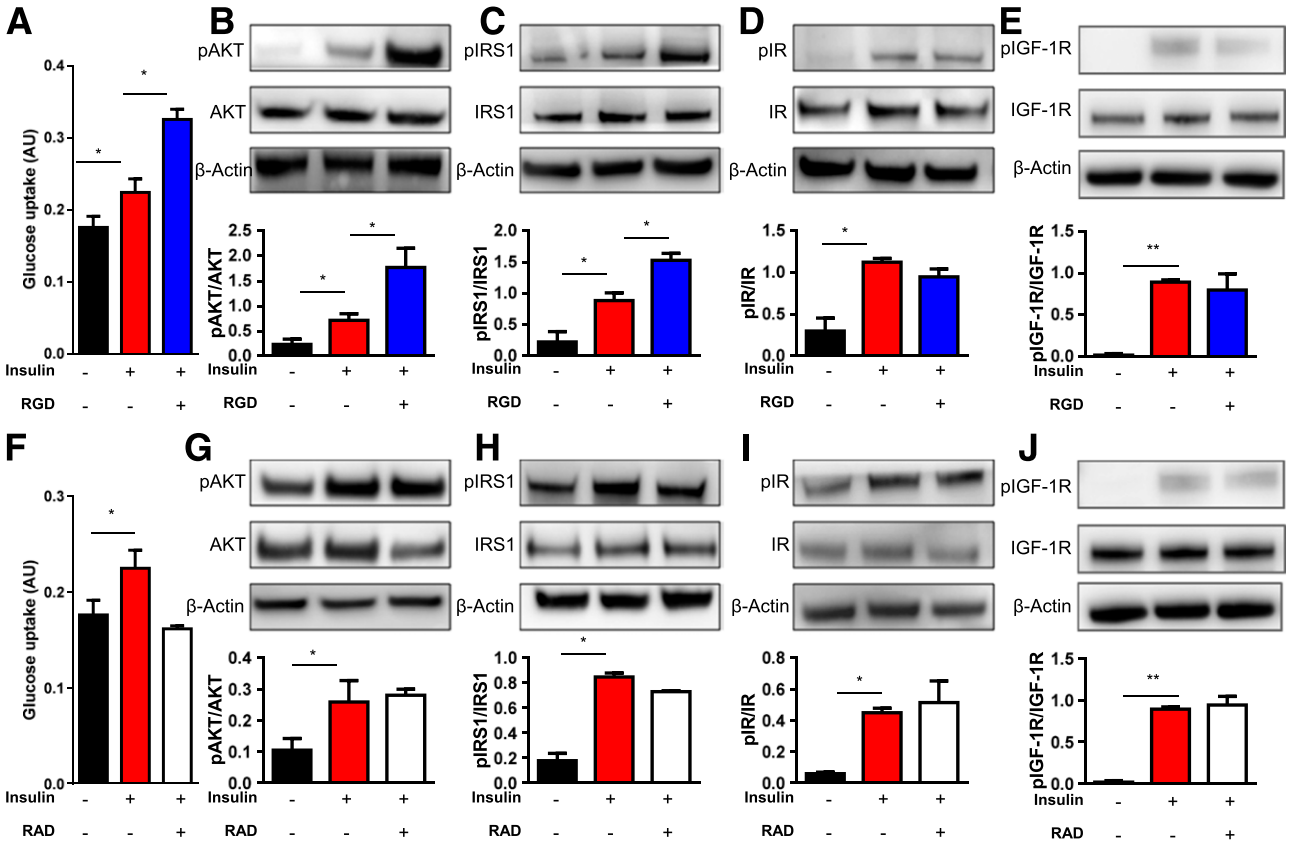

Figure 2—RGD synthetic peptide mimics rIGFBP-1–enhanced insulin signaling in C2C12 skeletal muscle cells. C2C12 myotubes were used to investigate the effects of RGD synthetic peptide on glucose uptake and the insulin signaling pathway. *A*: Pretreatment with RGD synthetic peptide increased insulin-stimulated glucose uptake compared with cells treated with insulin only (0.22 ± 0.02 vs. 0.33 ± 0.01 arbitrary units [AU]). *B–E*: Pretreatment with 500 ng/mL RGD synthetic hexapeptide for 10 min before 100 nmol/L insulin stimulation for 10 min caused an increase in insulin-stimulated pAKT/AKT and pIRS1/IRS1 but not pIR/IR or pIGF-1R/IGF-1R compared with cells treated with insulin only. *F*: Pretreatment with RAD control peptide did not increase insulin-stimulated glucose uptake compared with cells treated with insulin only (0.22 ± 0.02 vs. 0.16 ± 0.003 AU). *G–J*: Pretreatment with 500 ng/mL RAD control hexapeptide for 10 min before 100 nmol/L insulin stimulation for 10 min had no effect on insulin-stimulated pAKT/AKT, pIRS1/IRS1, pIR/IR, or pIGF-1R/IGF-1R compared with cells treated with insulin only. Data are mean ± SEM. $^*P \leq 0.05$, $^{**}P \leq 0.01$ ($n = 3$ for blots and $n = 8$ for uptake assays per treatment).

phosphorylation of AKT in gastrocnemius muscle in mice receiving RGD peptide was observed compared with mice receiving RAD control peptide (Fig. 5*H* and *I*).

Chronic RGD Peptide Treatment Had No Effect on Body Composition But Improved Insulin Sensitivity In Vivo

To examine whether chronic administration of RGD hexapeptide favorably affected metabolic homeostasis, we implanted osmotic minipumps delivering RGD peptide or RAD control peptide at 1 μg/h for 4 weeks. Minipumps were implanted in 12-week-old C57BL/6 mice fed a high-fat diet for 4 weeks. High-fat feeding was continued for a further 4 weeks during peptide infusion, after which metabolic profiling was performed. Chronic infusion of RGD peptide had no effect on body mass, lean mass, or adiposity (Fig. 6*A–C*). No difference in average energy expenditure, food intake, or water intake was found between the two groups (Fig. 6*D–F*). Circulating concentrations of IGF-I and IGFBP-1 were unaltered by RGD peptide administration (Supplementary Fig. 3). Furthermore, no difference in fasting blood glucose (Fig. 6*G*) was observed, but RGD peptide–infused mice had lower circulating plasma insulin levels than mice infused with RAD control peptide (Fig. 6*H*), consistent with enhanced insulin sensitivity. In keeping with a more insulin sensitive metabolic phenotype, RGD peptide–infused mice had lower HOMA of insulin resistance (HOMA-IR) scores than mice infused with RAD control peptide (Fig. 6*I*).

To examine the effects of chronic RGD peptide infusion on metabolic phenotype in more detail, hyperinsulinemic-euglycemic clamping was performed on obese C57BL/6 mice that had received RGD peptide or RAD control peptide through osmotic minipump for 4 weeks as described above. Euglycemia was reasonably well maintained during the clamp, with the exception of higher blood glucose in RGD peptide–infused mice at 70 and 90 min, resulting in a higher area under the curve (AUC) in these mice (Fig. 7*A* and *B*). Glucose infusion rate during the clamp was not significantly different at any time point, but a strong

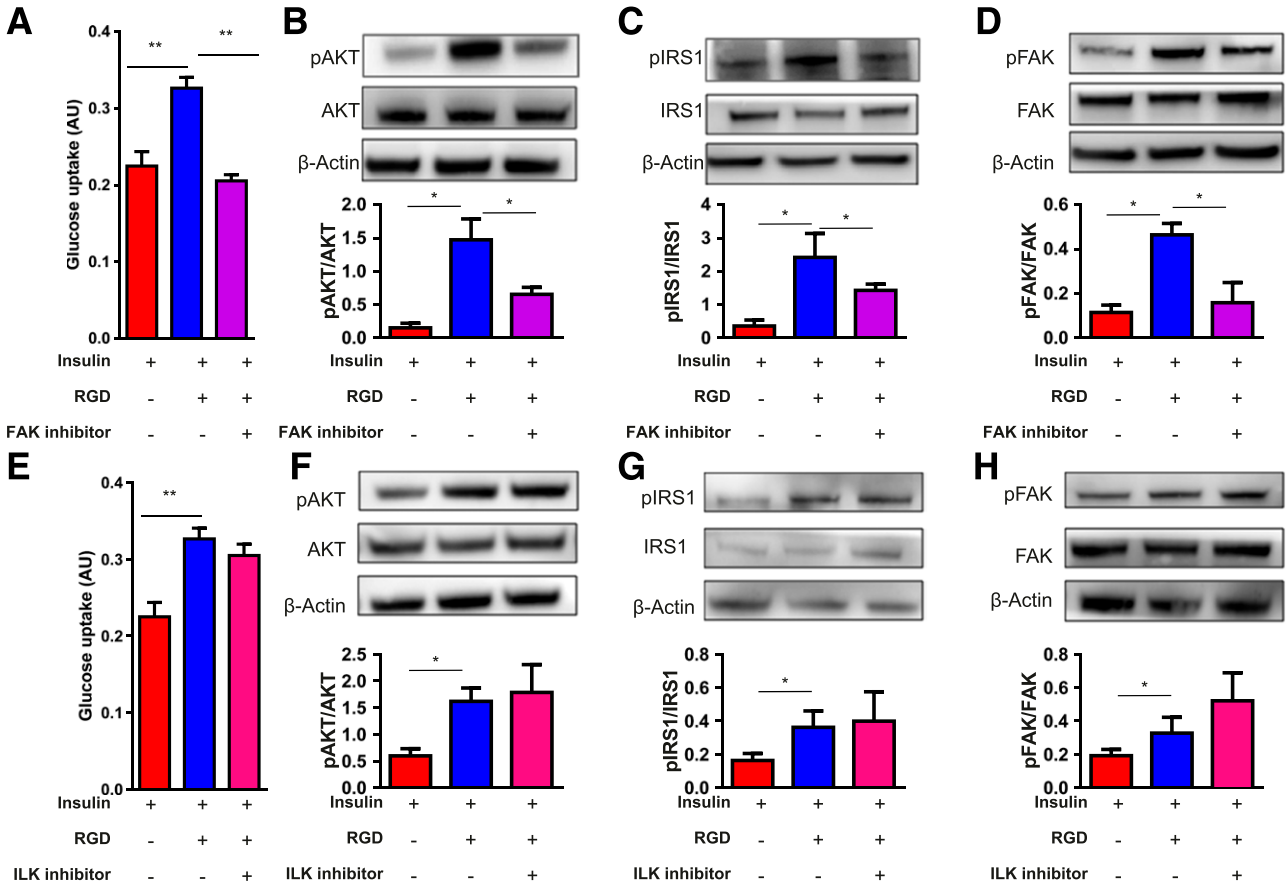

Figure 3—RGD synthetic peptide–enhanced insulin signaling in skeletal muscle cells is mediated by FAK. C2C12 myotubes were used to investigate the effects of RGD synthetic peptide on glucose uptake, insulin signaling, and FAK signaling. *A*: Pretreatment with RGD synthetic peptide after FAK inhibition but before insulin stimulation prevented RGD synthetic peptide–enhanced glucose uptake (0.33 ± 0.01 vs. 0.2 ± 0.008 arbitrary units [AU]). *B–D*: Pretreatment with RGD synthetic peptide after FAK inhibition but before insulin stimulation prevented RGD synthetic peptide–enhanced pAKT/AKT, pIRS1/IRS1, and pFAK/FAK. *E*: Pretreatment with RGD synthetic peptide after ILK inhibition but before insulin stimulation had no significant effect on RGD synthetic peptide–enhanced glucose uptake (0.33 ± 0.01 vs. 0.3 ± 0.02 AU). *F–H*: Pretreatment with RGD synthetic peptide after ILK inhibition but before insulin stimulation did not prevent RGD synthetic peptide–enhanced pAKT/AKT, pIRS1/IRS1, and pFAK/FAK. Data are mean ± SEM. *$P \leq 0.05$, **$P \leq 0.01$ ($n = 3$ for blots and $n = 8$ for uptake assays per treatment).

trend existed for RGD peptide–infused mice to require less glucose after 80 min of the clamp when steady state had been reached (Fig. 7*C*). Of note, plasma insulin during the clamp was significantly lower in RGD peptide–infused mice than in RAD control peptide–infused mice (Fig. 7*D*). In an attempt to control for the substantially lower insulin levels in RGD peptide–infused mice, we normalized glucose flux readouts for ambient insulin levels. Glucose disappearance relative to circulating insulin levels were increased in RGD peptide–infused mice compared with the RAD control peptide–infused mice (Fig. 7*E*). A trend to higher glucose uptake in muscle, particularly within the gastrocnemius; in white adipose tissue; and in the heart was observed in the RGD peptide–infused mice compared with RAD control peptide–infused mice (Fig. 7*F–H*). Glucose uptake in the brain and in brown adipose tissue was significantly enhanced in RGD peptide–infused mice as well (Fig. 7*H*).

To examine whether the metabolic phenotype of RGD peptide–infused mice was affected by changes in counterregulatory hormones, we measured circulating levels of growth hormone and glucagon at the end of the infusion period. Growth hormone and glucagon concentrations were similar in RGD peptide– and RAD control peptide–infused animals (Supplementary Fig. 3). Similarly, we found no difference in hepatic expression of $\alpha_5\beta_1$-integrin or of the gluconeogenic enzyme phosphoenolpyruvate carboxykinase between groups (Supplementary Fig. 4).

DISCUSSION

For the first time to our knowledge, this report demonstrates through a series of in vitro mechanistic studies that IGFBP-1 directly enhances insulin sensitivity through its RGD domain and that an RGD synthetic peptide enhances insulin secretion. By administering an RGD-containing hexapeptide in vivo, this study also shows that

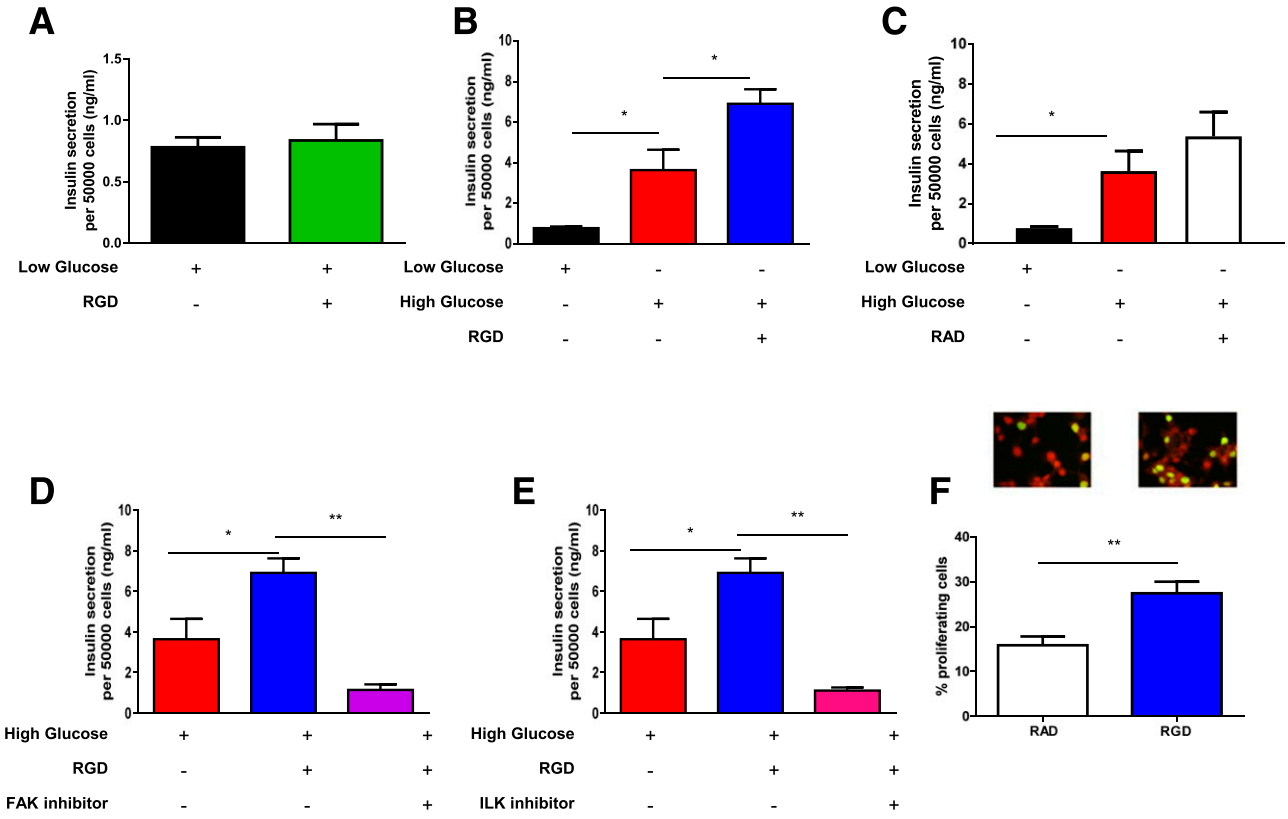

Figure 4—RGD synthetic hexapeptide enhances glucose-stimulated insulin secretion in pancreatic β-cells. INS-1 823/13, a pancreatic β-cell line, was used to investigate the effects of RGD synthetic peptide on insulin secretion. *A*: Coincubation with RGD synthetic peptide and low glucose had no effect on insulin secretion compared with cells treated with low glucose only (0.78 ± 0.08 vs. 0.83 ± 0.1 ng/mL). *B*: INS-1 823/13 was also used to investigate the effects of RGD synthetic peptide on glucose-stimulated insulin secretion. Coincubation with RGD synthetic peptide and glucose enhanced glucose-stimulated insulin secretion compared with cells treated with glucose only (3.64 ± 1 vs. 6.0 ± 0.7 ng/mL). *C*: Coincubation with RAD synthetic peptide and glucose had no effect on glucose-stimulated insulin secretion compared with cells treated with glucose only (3.64 ± 1 vs. 5.38 ± 1.2 ng/mL). *D*: Coincubation with FAK inhibitor, RGD synthetic peptide, and glucose prevented RGD-enhanced glucose-stimulated insulin secretion (6 ± 0.7 vs. 1.4 ± 0.3 ng/mL). *E*: Coincubation with ILK inhibitor, RGD synthetic peptide, and glucose prevented RGD-enhanced glucose-stimulated insulin secretion (6 ± 0.7 vs. 1.1 ± 0.15 ng/mL). *F*: INS-1 823/13 was used to investigate the effects of RGD synthetic peptide on proliferation by using a 5-ethynyl-2′-deoxyuridine assay. RGD synthetic peptide incubation for 2 h enhanced pancreatic β-cell proliferation compared with cells treated with the RAD control synthetic hexapeptide (RGD 27.45 ± 2.6% vs. RAD 15.8 ± 2%). Data are mean ± SEM. *$P \leq 0.05$, **$P \leq 0.01$ ($n = 4$ for secretion assays and $n = 8$ for proliferation assays).

this may be a potential novel therapeutic strategy to improve glucose tolerance and insulin sensitivity.

Skeletal muscle is the primary tissue responsible for postprandial (insulin-stimulated) glucose disposal that results from the activation of canonical signaling pathways leading to the translocation of GLUT4 to the cell surface membranes (36). Incubation of C2C12 myotubes, an insulin-sensitive cell type, with rIGFBP-1 caused a significant increase in insulin-stimulated IRS1 and AKT phosphorylation. These findings indicate that IGFBP-1 enhances signaling at critical nodes of the insulin signaling pathway. IGFBP-1 did not influence insulin-stimulated phosphorylation of the IR or IGF-1R, indicating that its potentiating effect on insulin signaling is mediated downstream of receptor tyrosine kinase activation.

Previous reports have indicated that IGFBP-1 can influence the function of a variety of cell types through interaction of its RGD domain with cell surface $\alpha_5\beta_1$-integrin (23–25,33). To determine whether this mechanism was responsible for the potentiating effect of IGFBP-1 on signaling in insulin-responsive cells, a mutant form of IGFBP-1 (WGD) that is incapable of binding $\alpha_5\beta_1$-integrin (23) was used. We confirmed that C2C12 cells express $\alpha_5\beta_1$-integrin. No increase in insulin signaling was seen when C2C12 cells were incubated with WGD-IGFBP-1. To further confirm the role of the RGD domain in insulin sensitization, we examined the effects of an RGD-containing peptide on insulin signaling. Although often used as competitive inhibitors at integrin receptors, RGD peptides can act as partial agonists and can stimulate integrin-mediated effects (37–39). We selected the linear RGD mimetic peptide GRGDTP because this replicated the effects of IGFBP-1 on integrin signaling and induction of apoptosis in breast cancer cells in a previous study (24). Enhanced insulin-stimulated phosphorylation of IRS1 and

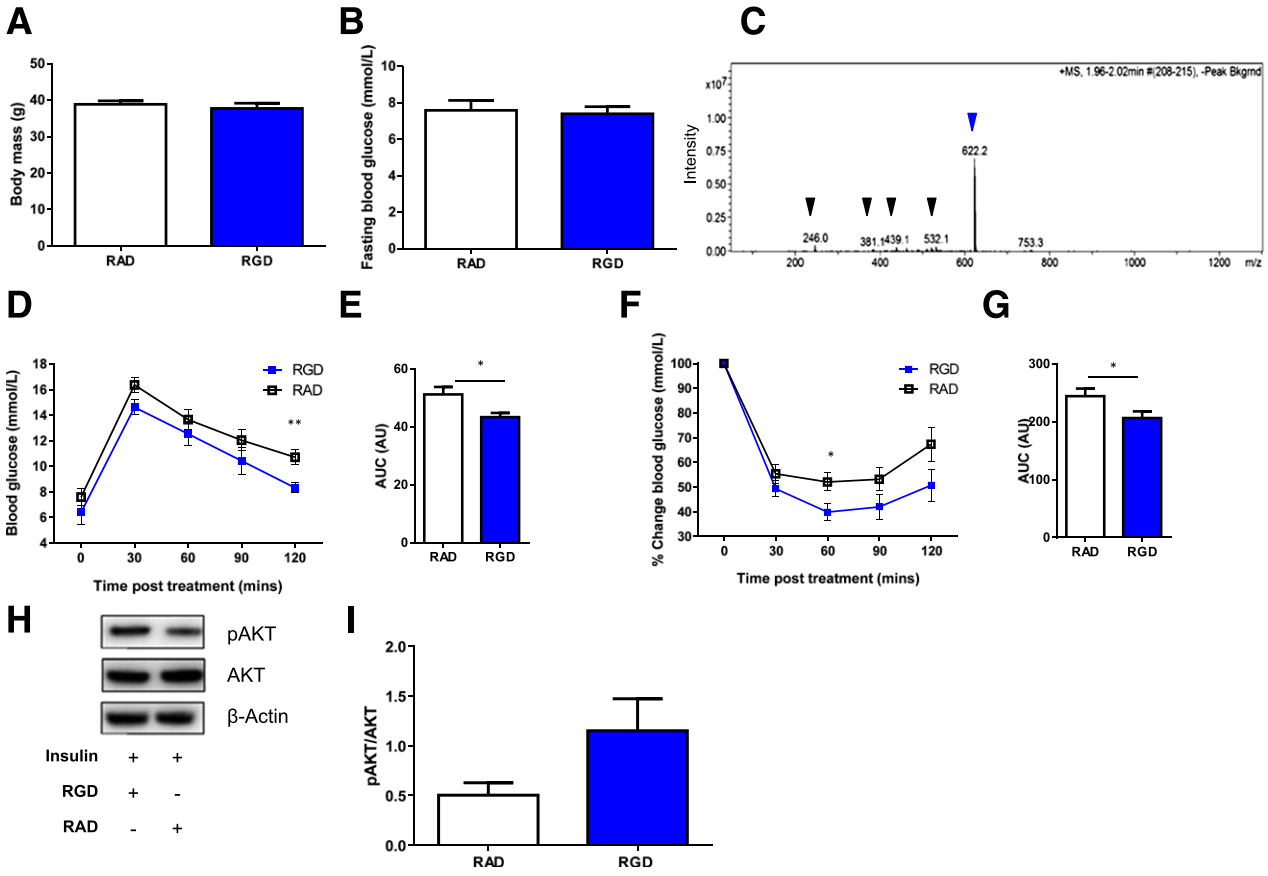

Figure 5—Acute RGD synthetic hexapeptide treatment improves glucose clearance and insulin sensitivity in obese C57BL/6 mice. Obese C57BL/6 mice were used to investigate the effect of acute RGD synthetic peptide injection. *A*: Body mass before injection was matched between groups (RGD 37.8 ± 1.4 vs. RAD 38.9 ± 0.97 g). *B*: Fasting blood glucose before injection was matched between groups (RGD 7.4 ± 0.4 vs. RAD 7.6 ± 0.5 mmol/L). *C*: Mass spectrometry identified the presence of the RGD synthetic hexapeptide (▼) in the blood and its metabolites (proteolytic fragments) (blue ▼) 30 min after intraperitoneal injection. Expected Electrospray Ionisation Mass Spectrometry (ESI MS) m/z 601 [M+H]+ or 624 [M+H]+ with an Na+ adduct of the peptide. ESI MS m/z 622.2 [M+H]+ due to fragmentation patterns arising from the isotopic distribution. *D* and *E*: Change in blood glucose levels after an intraperitoneal injection of RGD or RAD control synthetic peptide and glucose showed that 120 min postinjection, RGD-treated mice had significantly increased glucose clearance (RGD 8.3 ± 0.6 vs. RAD 10.7 ± 0.4 mmol/L), as also shown by the AUC analysis (RGD 43.3 ± 1.5 vs. RAD 51.2 ± 2.6 arbitrary units [AU]). *F* and *G*: Percentage change in blood glucose levels after an intraperitoneal injection of RGD or RAD control synthetic peptide and insulin showed that mice treated with RGD peptide were significantly more insulin sensitive at 60 min (RGD 39.8 ± 3.4 vs. RAD 52 ± 3.7%), as also shown by the AUC analysis (RGD 206.4 ± 11.6 vs. RAD 244.1 ± 13 AU). *H* and *I*: Western blot representative images and graphical representations of pAKT and AKT from ex vivo gastrocnemius muscle after stimulation with either insulin and RGD or insulin and RAD ($P = 0.09$). Data are mean ± SEM. $^*P \leq 0.09$, $^{**}P \leq 0.01$ ($n = 10$/group). m/z, charge/mass ratio.

AKT was reproduced by the RGD peptide, although at a higher molar concentration, suggesting that the peptide is less active than intact IGFBP-1 protein. Insulin signaling was not affected by the RAD control peptide, providing further evidence that the insulin-sensitizing effects of IGFBP-1 are mediated through its integrin-binding domain.

Evidence now suggests that the extracellular matrix plays a critical role in modulating insulin action (40). Cell surface integrins, which interact with matrix components and communicate with intracellular signaling pathways, are intricately involved with modulating insulin sensitivity. Accordingly, mice lacking β_1-integrin in skeletal muscle exhibit marked insulin resistance (41). The cytoplasmic domains of integrins interact with intermediaries such as FAK, which plays a critical role in modulating insulin sensitivity and glucose tolerance (42–44). Consistent with a report that FAK is activated by IGFBP-1 in human breast cancer cells (24), we show that RGD peptide increases insulin-stimulated FAK phosphorylation in C2C12 skeletal myotubes. Inhibition of FAK prevents the RGD peptide from enhancing insulin signaling and cellular glucose uptake, indicating that FAK plays an essential role in mediating the insulin-sensitizing effects of RGD. Consistent with the enhanced insulin signaling observed in the current study, FAK interacts with IRS1, at which point integrin and IR signaling pathways converge, ultimately stimulating glucose uptake (44–46).

T2DM is characterized not only by systemic insulin resistance but also by decompensation of the pancreatic β-cells that secrete insulin in response to increased blood

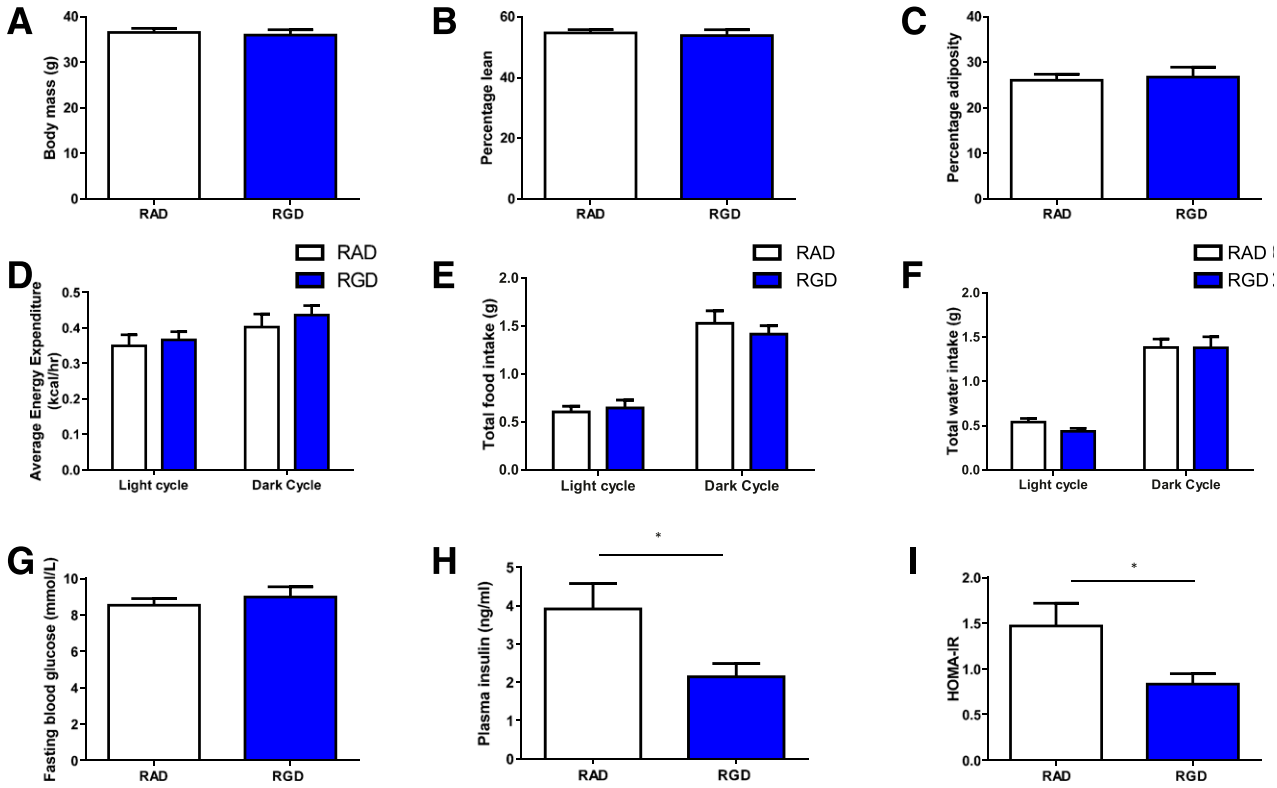

Figure 6—Chronic RGD synthetic hexapeptide treatment has no effect on body composition but improves insulin resistance in obese C57BL/6 mice. Obese C57BL/6 mice were used to investigate the effect of chronic RGD synthetic peptide infusion through osmotic minipump. *A*: Body mass after 4 weeks of infusion was not different between groups (RGD 36 ± 1.2 vs. RAD 36.6 ± 0.9 g). *B*: No difference was found in percentage lean mass between the groups (RGD 53.9 ± 1.9 vs. RAD 54.7 ± 1.1%). *C*: No difference was found in adiposity (RGD 26.8 ± 2.2 vs. RAD 26.1 ± 1.3%). *D*: No difference was found in average energy expenditure between the groups during the light cycle (RGD 0.37 ± 0.02 vs. RAD 0.35 ± 0.03 kcal/h) and dark cycle (RGD 0.44 ± 0.03 vs. RAD 0.4 ± 0.04 kcal/h). *E*: There was no difference in food intake between the groups during the light cycle (RGD 0.65 ± 0.08 vs. RAD 0.61 ± 0.06 g) and dark cycle (RGD 1.53 ± 0.09 vs. RAD 1.42 ± 0.13 g). *F*: No difference was found in water intake between the two groups during the light cycle (RGD 0.44 ± 0.004 vs. RAD 0.54 ± 0.004 g) and dark cycle (RGD 1.39 ± 0.003 vs. RAD 1.39 ± 0.002 g). *G*: There was no difference in fasting blood glucose (RGD 8.98 ± 0.57 vs. RAD 8.54 ± 0.36 mmol/L). *H*: RGD-infused mice had lower circulating plasma insulin levels compared with mice that received the RAD control peptide (RGD 2.1 ± 0.34 vs. RAD 3.9 ± 0.67 ng/mL). *I*: RGD-infused mice had lower HOMA-IR scores than mice that received RAD control peptide (RGD 0.8 ± 0.11 vs. RAD 1.5 ± 0.25). Data are mean ± SEM. $^*P \leq 0.05$ (n = 8/group).

glucose levels. Previously, IGFBP-1 has been reported to amplify glucose-stimulated insulin secretion in intact islets (47). This appeared to be mediated indirectly through reduced somatostatin secretion because IGFBP-1 inhibited glucose-stimulated insulin secretion in isolated mouse β-cells (44). In contrast, we showed that treatment of INS-1 823/13 cells, a glucose-responsive pancreatic β-cell line, with RGD peptide enhanced glucose-induced insulin secretion (47). The discrepant results may reflect differences between IGFBP-1 and RGD peptide as ligands or the different cell types used in these studies. The findings agree with a previous study in which INS-1 cells grown on plates coated with an RGD peptide exhibited higher glucose-stimulated insulin secretion than those grown on tissue culture plastic (48). We also found that RGD peptide increased proliferation of INS-1 823/13 cells compared with those treated with the RAD control peptide. FAK-dependent remodeling of focal adhesions in pancreatic β-cells plays an integral role in glucose-stimulated insulin secretion (49,50). Of note, we found that both FAK and ILK were involved in mediating enhanced glucose-stimulated insulin secretion in response to RGD peptide. In keeping with a role in islet cell function, ILK has been shown to extend the duration of viability and insulin secretion in MIN6 cells (51).

To determine whether the effects of the RGD peptide on insulin sensitivity and pancreatic insulin secretion in vitro were also apparent in vivo, we carried out metabolic phenotyping of diet-induced obese mice after administration of the peptide. RGD-containing peptides have been widely investigated clinically as antiangiogenic agents in cancer and for molecular targeting of drugs or imaging probes (52,53). However, potential effects of RGD-containing peptides on glucose homeostasis in vivo have not been explored.

Acute administration of RGD peptide to obese C57BL/6 mice led to significant improvement in both glucose tolerance and insulin sensitivity in vivo. Chronic infusion

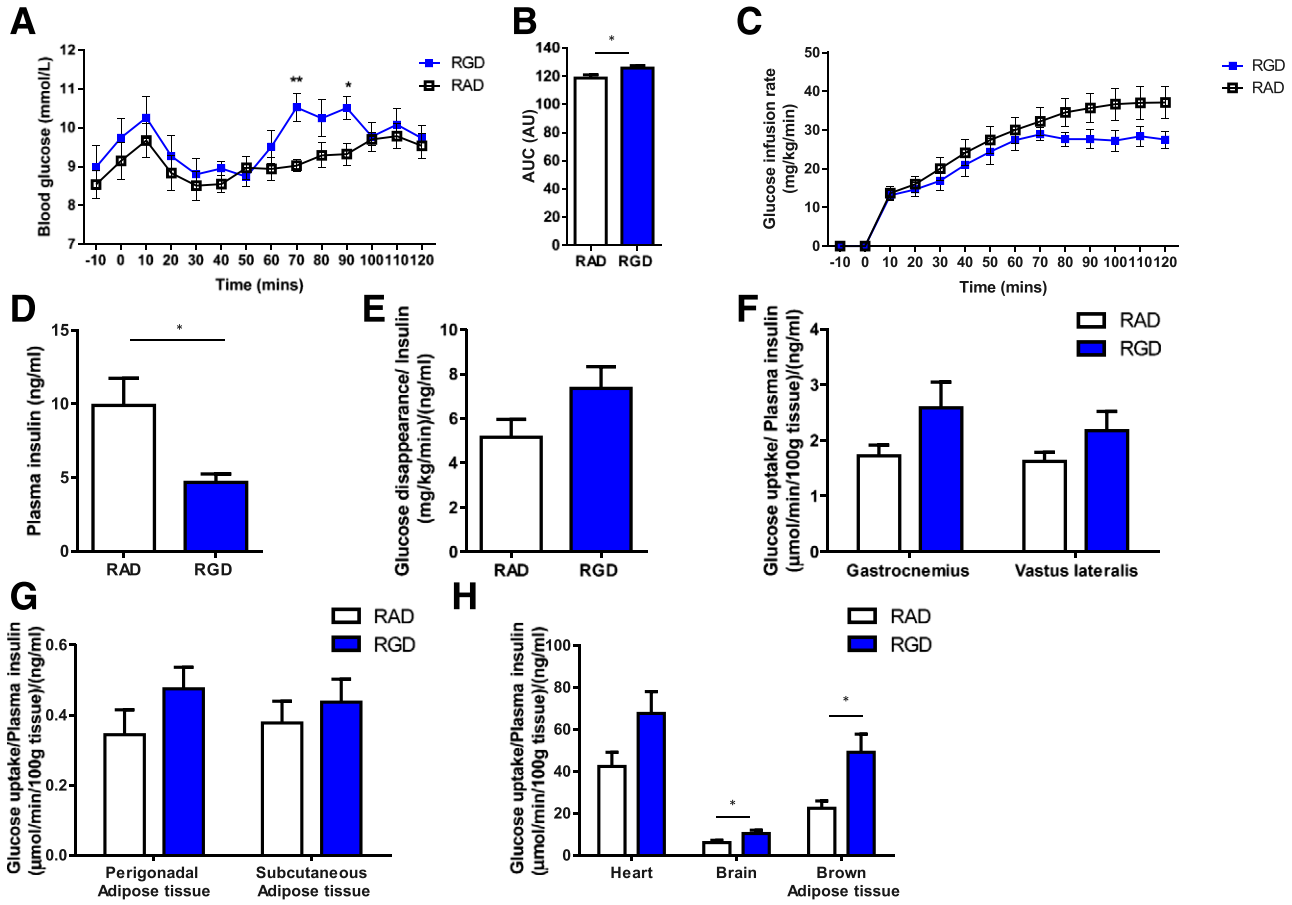

Figure 7—Chronic RGD synthetic hexapeptide treatment enhances glucose in obese C57BL/6 mice. Hyperinsulinemic-euglycemic clamping was performed on obese C57BL/6 mice that received RGD synthetic peptide or RAD control peptide infusion through osmotic minipump for 4 weeks. *A* and *B*: Blood glucose during the clamp at 70 and 90 min in RGD-treated mice was significantly higher than in RAD control–treated mice (70 min: RGD 10.5 ± 0.36 vs. RAD 9 ± 0.15 mmol/L; 90 min: RGD 10.5 ± 0.3 vs. RAD 9.3 ± 0.3 mmol/L), and the AUC analysis for these was significantly different (RGD 125.8 ± 1.8 vs. RAD ± 2.6 arbitrary units [AU]). *C*: Glucose infusion rate during the clamp was not significantly different. *D*: Plasma insulin during the clamp was significantly lower in RGD-treated mice compared with RAD control peptide–treated mice (RGD 4.7 ± 0.6 vs. RAD 9.9 ± 1.8 ng/mL). *E*: Glucose disappearance relative to circulating insulin levels was not significantly different between the groups [RGD 7.4 ± 1 vs. RAD 5.2 ± 0.8 (mg/kg/min)/(ng/mL); $P = 0.1$]. *F*: Glucose uptake in muscle was not significantly different between the groups [gastrocnemius: RGD 2.6 ± 0.5 vs. RAD 1.7 ± 0.2 (µmol/min/100 g tissue)/(ng/mL) ($P = 0.09$); vastus lateralis: RGD 2.2 ± 0.4 vs. RAD 1.6 ± 0.2 (µmol/min/100 g tissue)/(ng/mL)]. *G*: Glucose uptake in white adipose tissue was not significantly different between the groups [perigonadal adipose tissue: RGD 0.48 ± 0.07 vs. RAD 0.35 ± 0.06 (µmol/min/100 g tissue)/(ng/mL); subcutaneous adipose tissue: RGD 0.44 ± 0.07 vs. RAD 0.38 ± 0.08 (µmol/min/100 g tissue)/(ng/mL)]. *H*: Glucose uptake in heart was not significantly different between the groups [RGD 67.63 ± 10.4 vs. RAD 42.4 ± 6.7 (µmol/min/100 g tissue)/(ng/mL)], but glucose uptake in the brain and in brown adipose tissue was significantly increased in RGD peptide–infused mice compared with RAD control peptide–infused mice [brain: RGD 10.5 ± 1.5 vs. RAD 6.1 ± 1.1 (µmol/min/100 g tissue)/(ng/mL); brown adipose tissue: RGD 49.1 ± 9.3 vs. RAD 22.5 ± 10 (µmol/min/100 g tissue)/(ng/mL)]. Data are mean ± SEM. *$P \leq 0.05$, **$P \leq 0.01$ (n = 8/group).

of RGD peptide for 4 weeks in obese mice was well tolerated with no effect on body composition or energy expenditure. Fasting blood glucose levels were unaffected by RGD peptide infusion, but fasting insulin concentrations were lower in RGD peptide–infused mice consistent with insulin sensitization. An insulin-sensitive phenotype was supported by a lower HOMA-IR score in RGD peptide–infused mice. In hyperinsulinemic-euglycemic clamp studies, we did not identify a significance difference in glucose infusion rate between RGD peptide– and RAD control peptide–treated mice. However, plasma insulin concentrations were substantially lower during the clamp in the RGD peptide–infused animals. Although the reason for this cannot be inferred from the clamp data, increased insulin clearance by the liver and kidney or decreased pancreatic insulin secretion in vivo may have contributed to the lower insulin levels in RGD-treated mice. RGD peptide infusion did not alter the expression of integrins or gluconeogenic enzymes in liver. We did not find any difference in counterregulatory hormones (e.g., glucagon, growth hormone) between animals.

In contrast to our findings in C2C12 cells exposed to RGD peptide in vitro, we did not observe a statistically significant difference in glucose uptake in vivo. However, in contrast to the in vitro studies in which the concentration of insulin was standardized across experiments,

interpretation of the in vivo data is confounded by the substantial difference in circulating insulin levels achieved during the clamp. In an attempt to correct for the different ambient insulin levels, we normalized glucose flux data to plasma insulin concentrations and identified a trend for increased glucose disposal and glucose uptake into gastrocnemius muscle and significantly increased glucose uptake in brain and brown adipose tissue in RGD peptide–infused mice.

Collectively, the current in vitro and in vivo data suggest a direct insulin-sensitizing effect of IGFBP-1 mediated at the cellular level through RGD-integrin interaction and activation of FAK. This may serve as an important mechanism by which IGFBP-1 contributes to glucose homeostasis and modulates susceptibility to T2DM independent of its known role in regulating the bioavailability of IGFs. For the first time, we have shown that rIGFBP-1, by way of its RGD domain, through $\alpha_5\beta_1$-integrin and subsequent FAK activation increases insulin sensitivity through the AKT signaling pathway in skeletal muscle cells, and that, in turn, increases glucose uptake. RGD peptides also improve glucose-stimulated insulin secretion from pancreatic β-cells through FAK and ILK activation. Promising improvements in glucose tolerance and insulin sensitivity elicited in vivo suggest that IGFBP-1 and its RGD domain are potential novel therapeutic candidates in the field of T2DM.

Acknowledgments. The authors thank Rajendra Gosain (University of Leeds) for assistance with the mass spectrometry analysis.

Funding. N.J.H. was funded by a British Heart Foundation PhD studentship. M.T.K. holds a British Heart Foundation Chair in Cardiology. S.B.W. is supported by a European Research Council Starting Grant.

Duality of Interest. No potential conflicts of interest relevant to this article were reported.

Author Contributions. N.J.H. designed and performed the in vitro and in vivo experiments, analyzed data, and wrote the manuscript. P.A.C., K.Y.T., H.I., H.V., and A.F.B. performed the in vitro experiments and reviewed the manuscript. N.M. and N.Y.Y. performed the in vivo studies. R.M.C., M.T.K., and S.B.W. conceived the study, obtained funding, designed the experiments, supervised the project, and reviewed the manuscript. S.B.W. is the guarantor of the work and, as such, had full access to all the data in the study and takes responsibility for the integrity of the data and the accuracy of the data analysis.

References

1. Finucane MM, Stevens GA, Cowan MJ, et al.; Global Burden of Metabolic Risk Factors of Chronic Diseases Collaborating Group (Body Mass Index). National, regional, and global trends in body-mass index since 1980: systematic analysis of health examination surveys and epidemiological studies with 960 country-years and 9.1 million participants. Lancet 2011;377:557–567

2. Wild S, Roglic G, Green A, Sicree R, King H. Global prevalence of diabetes: estimates for the year 2000 and projections for 2030. Diabetes Care 2004;27:1047–1053

3. Booth GL, Kapral MK, Fung K, Tu JV. Relation between age and cardiovascular disease in men and women with diabetes compared with non-diabetic people: a population-based retrospective cohort study. Lancet 2006;368:29–36

4. Tahrani AA, Bailey CJ, Del Prato S, Barnett AH. Management of type 2 diabetes: new and future developments in treatment. Lancet 2011;378:182–197

5. Gerstein HC, Miller ME, Byington RP, et al.; Action to Control Cardiovascular Risk in Diabetes Study Group. Effects of intensive glucose lowering in type 2 diabetes. N Engl J Med 2008;358:2545–2559

6. Firth SM, Baxter RC. Cellular actions of the insulin-like growth factor binding proteins. Endocr Rev 2002;23:824–854

7. Brismar K, Fernqvist-Forbes E, Wahren J, Hall K. Effect of insulin on the hepatic production of insulin-like growth factor-binding protein-1 (IGFBP-1), IGFBP-3, and IGF-I in insulin-dependent diabetes. J Clin Endocrinol Metab 1994;79:872–878

8. Wheatcroft SB, Kearney MT. IGF-dependent and IGF-independent actions of IGF-binding protein-1 and -2: implications for metabolic homeostasis. Trends Endocrinol Metab 2009;20:153–162

9. Heald AH, Cruickshank JK, Riste LK, et al. Close relation of fasting insulin-like growth factor binding protein-1 (IGFBP-1) with glucose tolerance and cardiovascular risk in two populations. Diabetologia 2001;44:333–339

10. Gokulakrishnan K, Velmurugan K, Ganesan S, Mohan V. Circulating levels of insulin-like growth factor binding protein-1 in relation to insulin resistance, type 2 diabetes mellitus, and metabolic syndrome (Chennai Urban Rural Epidemiology Study 118). Metabolism 2012;61:43–46

11. Liew CF, Wise SD, Yeo KP, Lee KO. Insulin-like growth factor binding protein-1 is independently affected by ethnicity, insulin sensitivity, and leptin in healthy, glucose-tolerant young men. J Clin Endocrinol Metab 2005;90:1483–1488

12. Rajpathak SN, McGinn AP, Strickler HD, et al. Insulin-like growth factor-(IGF)-axis, inflammation, and glucose intolerance among older adults. Growth Horm IGF Res 2008;18:166–173

13. Mogul HR, Marshall M, Frey M, et al. Insulin like growth factor-binding protein-1 as a marker for hyperinsulinemia in obese menopausal women. J Clin Endocrinol Metab 1996;81:4492–4495

14. Mohamed-Ali V, Pinkney JH, Panahloo A, Cwyfan-Hughes S, Holly JM, Yudkin JS. Insulin-like growth factor binding protein-1 in NIDDM: relationship with the insulin resistance syndrome. Clin Endocrinol (Oxf) 1999;50:221–228

15. Travers SH, Labarta JI, Gargosky SE, Rosenfeld RG, Jeffers BW, Eckel RH. Insulin-like growth factor binding protein-I levels are strongly associated with insulin sensitivity and obesity in early pubertal children. J Clin Endocrinol Metab 1998;83:1935–1939

16. Saitoh H, Kamoda T, Nakahara S, Hirano T, Nakamura N. Serum concentrations of insulin, insulin-like growth factor(IGF)-I, IGF binding protein (IGFBP)-1 and -3 and growth hormone binding protein in obese children: fasting IGFBP-1 is suppressed in normoinsulinaemic obese children. Clin Endocrinol (Oxf) 1998;48:487–492

17. Sandhu MS, Heald AH, Gibson JM, Cruickshank JK, Dunger DB, Wareham NJ. Circulating concentrations of insulin-like growth factor-I and development of glucose intolerance: a prospective observational study. Lancet 2002;359:1740–1745

18. Lewitt MS, Hilding A, Ostenson C-G, Efendic S, Brismar K, Hall K. Insulin-like growth factor-binding protein-1 in the prediction and development of type 2 diabetes in middle-aged Swedish men. Diabetologia 2008;51:1135–1145

19. Petersson U, Ostgren CJ, Brudin L, Brismar K, Nilsson PM. Low levels of insulin-like growth-factor-binding protein-1 (IGFBP-1) are prospectively associated with the incidence of type 2 diabetes and impaired glucose tolerance (IGT): the Söderåkra Cardiovascular Risk Factor Study. Diabetes Metab 2009;35:198–205

20. Rajpathak SN, He M, Sun Q, et al. Insulin-like growth factor axis and risk of type 2 diabetes in women. Diabetes 2012;61:2248–2254

21. Wilson D; Glaser Pediatric Research Network Obesity Study Group. Intraperitoneal fat and insulin resistance in obese adolescents. Obesity (Silver Spring) 2010;18:402–409

22. Rajwani A, Ezzat V, Smith J, et al. Increasing circulating IGFBP1 levels improves insulin sensitivity, promotes nitric oxide production, lowers blood pressure, and protects against atherosclerosis. Diabetes 2012;61:915–924

23. Jones JI, Gockerman A, Busby WH Jr, Wright G, Clemmons DR. Insulin-like growth factor binding protein 1 stimulates cell migration and binds to the alpha 5 beta 1 integrin by means of its Arg-Gly-Asp sequence. Proc Natl Acad Sci U S A 1993;90:10553–10557

24. Perks CM, Newcomb PV, Norman MR, Holly JM. Effect of insulin-like growth factor binding protein-1 on integrin signalling and the induction of apoptosis in human breast cancer cells. J Mol Endocrinol 1999;22:141–150
25. Chesik D, De Keyser J, Bron R, Fuhler GM. Insulin-like growth factor binding protein-1 activates integrin-mediated intracellular signaling and migration in oligodendrocytes. J Neurochem 2010;113:1319–1330
26. Brandt K, Grünler J, Brismar K, Wang J. Effects of IGFBP-1 and IGFBP-2 and their fragments on migration and IGF-induced proliferation of human dermal fibroblasts. Growth Horm IGF Res 2015;25:34–40
27. Weir JB. New methods for calculating metabolic rate with special reference to protein metabolism. J Physiol 1949;109:1–9
28. Berglund ED, Li CY, Poffenberger G, et al. Glucose metabolism in vivo in four commonly used inbred mouse strains. Diabetes 2008;57:1790–1799
29. Ayala JE, Bracy DP, McGuinness OP, Wasserman DH. Considerations in the design of hyperinsulinemic-euglycemic clamps in the conscious mouse. Diabetes 2006;55:390–397
30. Finegood DT, Bergman RN, Vranic M. Estimation of endogenous glucose production during hyperinsulinemic-euglycemic glucose clamps. Comparison of unlabeled and labeled exogenous glucose infusates. Diabetes 1987;36:914–924
31. Steele R, Wall JS, De Bodo RC, Altszuler N. Measurement of size and turnover rate of body glucose pool by the isotope dilution method. Am J Physiol 1956;187:15–24
32. Kraegen EW, James DE, Jenkins AB, Chisholm DJ. Dose-response curves for in vivo insulin sensitivity in individual tissues in rats. Am J Physiol 1985;248: E353–E362
33. Galiano RD, Zhao LL, Clemmons DR, Roth SI, Lin X, Mustoe TA. Interaction between the insulin-like growth factor family and the integrin receptor family in tissue repair processes: evidence in a rabbit ear dermal ulcer model. J Clin Invest 1996;98:2462–2468
34. Harburger DS, Calderwood DA. Integrin signalling at a glance. J Cell Sci 2009;122:159–163
35. Zaidel-Bar R, Itzkovitz S, Ma'ayan A, Iyengar R, Geiger B. Functional atlas of the integrin adhesome. Nat Cell Biol 2007;9:858–867
36. Warram JH, Martin BC, Krolewski AS, Soeldner JS, Kahn CR. Slow glucose removal rate and hyperinsulinemia precede the development of type II diabetes in the offspring of diabetic parents. Ann Intern Med 1990;113:909–915
37. Legler DF, Wiedle G, Ross FP, Imhof BA. Superactivation of integrin alphavbeta3 by low antagonist concentrations. J Cell Sci 2001;114:1545–1553
38. Umesh A, Thompson MA, Chini EN, Yip KP, Sham JS. Integrin ligands mobilize Ca2+ from ryanodine receptor-gated stores and lysosome-related acidic organelles in pulmonary arterial smooth muscle cells. J Biol Chem 2006; 281:34312–34323
39. Reynolds AR, Hart IR, Watson AR, et al. Stimulation of tumor growth and angiogenesis by low concentrations of RGD-mimetic integrin inhibitors. Nat Med 2009;15:392–400
40. Williams AS, Kang L, Wasserman DH. The extracellular matrix and insulin resistance. Trends Endocrinol Metab 2015;26:357–366
41. Zong H, Bastie CC, Xu J, et al. Insulin resistance in striated muscle-specific integrin receptor beta1-deficient mice. J Biol Chem 2009;284:4679–4688
42. Guan JL. Role of focal adhesion kinase in integrin signaling. Int J Biochem Cell Biol 1997;29:1085–1096
43. Huang D, Khoe M, Ilic D, Bryer-Ash M. Reduced expression of focal adhesion kinase disrupts insulin action in skeletal muscle cells. Endocrinology 2006;147:3333–3343
44. Bisht B, Goel HL, Dey CS. Focal adhesion kinase regulates insulin resistance in skeletal muscle. Diabetologia 2007;50:1058–1069
45. Lebrun P, Mothe-Satney I, Delahaye L, Van Obberghen E, Baron V. Insulin receptor substrate-1 as a signaling molecule for focal adhesion kinase pp125(FAK) and pp60(src). J Biol Chem 1998;273:32244–32253
46. El Annabi S, Gautier N, Baron V. Focal adhesion kinase and Src mediate integrin regulation of insulin receptor phosphorylation. FEBS Lett 2001;507: 247–252
47. Zhang F, Sjöholm Å, Zhang Q. Attenuation of insulin secretion by insulin-like growth factor binding protein-1 in pancreatic beta-cells. Biochem Biophys Res Commun 2007;362:152–157
48. Kuehn C, Dubiel EA, Sabra G, Vermette P. Culturing INS-1 cells on CDPGYIGSR-, RGD- and fibronectin surfaces improves insulin secretion and cell proliferation. Acta Biomater 2012;8:619–626
49. Rondas D, Tomas A, Halban PA. Focal adhesion remodeling is crucial for glucose-stimulated insulin secretion and involves activation of focal adhesion kinase and paxillin. Diabetes 2011;60:1146–1157
50. Rondas D, Tomas A, Soto-Ribeiro M, Wehrle-Haller B, Halban PA. Novel mechanistic link between focal adhesion remodeling and glucose-stimulated insulin secretion. J Biol Chem 2012;287:2423–2436
51. Blanchette JO, Langer SJ, Sahai S, Topiwala PS, Leinwand LL, Anseth KS. Use of integrin-linked kinase to extend function of encapsulated pancreatic tissue. Biomed Mater 2010;5:061001
52. Danhier F, Le Breton A, Préat V. RGD-based strategies to target alpha(v) beta(3) integrin in cancer therapy and diagnosis. Mol Pharm 2012;9:2961–2973
53. Montet X, Funovics M, Montet-Abou K, Weissleder R, Josephson L. Multivalent effects of RGD peptides obtained by nanoparticle display. J Med Chem 2006;49:6087–6093